Proceedings of the AMS Centennial Symposium
August 8–12, 1988

Two Examples of Mathematics and Computing in the Biological Sciences: Blood Flow in the Heart and Molecular Dynamics

CHARLES S. PESKIN

Introduction. Mathematics plays a unifying role in the sciences, since diverse natural phenomena can often be described with the help of similar mathematical methods. This paper discusses two quite different biomathematical problems in which essentially the same issue of numerical stability can be resolved in essentially the same way: through the use of an implicit method that requires the solution of an optimization problem at each time step. In the case of blood flow in the heart, this leads to a computational method that can be used to study the normal and pathological function of the heart and also to predict the performance of proposed designs for prosthetic cardiac valves. In the case of molecular dynamics, the method described in this paper has the unexpected ability to simulate certain quantum-mechanical effects in an otherwise classical context. Moreover, this method should make it possible to use large time steps and thus to simulate slow molecular processes which have hitherto been beyond the reach of molecular dynamics.

The equations of cardiac fluid dynamics. Our purpose in this section is to give a new derivation of the equations that describe the mechanical function of the heart. These equations encompass the fluid mechanics of the blood, the passive elasticity of the heart valve leaflets, and the active (time-dependent) elasticity of the muscular heart walls. The entire system is incompressible, and we use the incompressible-elasticity approach of Ebin and Saxton [**1**, 2], which produces considerable simplification in the equations of nonlinear elasticity. This simplification is achieved through the strategic use of a mixed Lagrangian-Eulerian description of the motion.

One way to express the connection between these two descriptions is to use integral transformations in which the Dirac δ-function appears as a kernel.

1980 *Mathematics Subject Classification* (1985 *Revision*). Primary 92–08; Secondary 65L20, 65M12, 70H05, 70L05, 76Z05, 81–08, 81V55, 82B10, 82C31, 92C35, 92C40.

0-8218-0167-8 $1.00 + $.25 per page

We adopt this approach here, as it illuminates the path that we follow in the construction of a computational method for the solution of the equations derived in this section.

We begin with a Lagrangian description of the motion:

$$\mathbf{x} = \mathbf{X}(a, t), \tag{1}$$

where $a = (q, r, s)$ is a list of Lagrangian parameters, i.e., fixed a marks a material point. Let $m(a)da = m(q, r, s)dq\,dr\,ds$ be the mass of the material element da. Note that m is independent of time, since mass is conserved.

Let the elastic potential energy of the system be given by a functional $E[\ , t]$ which takes as input the function $\mathbf{X}(\ , t)$. The explicit time-dependence in E is what makes it possible for the heart to contract and relax. We shall denote by $-\mathbf{f}(a, t)$ the Fréchet derivative of E with respect to $\mathbf{X}$. This means that

$$\lim_{\varepsilon \to 0} \frac{d}{d\varepsilon} E[\mathbf{X} + \varepsilon \mathbf{Y}, t] = -\int \mathbf{f}(a, t) \cdot \mathbf{Y}(a)\, da \tag{2}$$

for all $\mathbf{Y}(a)$.

With the notation developed above, we may write down the Lagrangian of the system as

$$L(t) = \frac{1}{2} \int m(a) \left| \frac{\partial \mathbf{X}}{\partial t}(a, t) \right|^2 da - E[\mathbf{X}(\ , t), t]. \tag{3}$$

According to Hamilton's principle of least action, the actual motion $\mathbf{X}(a, t)$ is a stationary point of the action integral

$$S = \int_0^T L(t)\, dt. \tag{4}$$

This means that if the actual motion $\mathbf{X}(a, t)$ is embedded in a family of hypothetical motions $\mathbf{X}(a, t, \varepsilon)$, all of which are consistent with the constraints (see below) and in such a manner that $\mathbf{X}(a, t) = \mathbf{X}(a, t, 0)$, and if $S(\varepsilon)$ is the action corresponding to the hypothetical motion $\mathbf{X}(a, t, \varepsilon)$, then $dS/d\varepsilon = 0$ at $\varepsilon = 0$.

The constraints in question are as follows. First, we assume that the initial and final configurations of the material particles of the system are specified:

$$\mathbf{X}(a, 0, \varepsilon) = \mathbf{X}_0(a) \quad \text{(given)}, \tag{5}$$

$$\mathbf{X}(a, T, \varepsilon) = \mathbf{X}_T(a) \quad \text{(given)}. \tag{6}$$

Next, we assume that the motions under consideration are all volume-preserving. This means that for any region A in parameter space and for all (t, ε), we have

$$\text{volume}(\mathbf{X}(A, t, \varepsilon)) = \text{volume}(\mathbf{X}_0(A)). \tag{7}$$

This is the same as saying that

$$\det\left(\frac{\partial \mathbf{X}}{\partial a}(a, t, \varepsilon)\right) = J_0(a) \tag{8}$$

independent of t and ε. This completes the statement of the constraints.

Evaluating $S(\varepsilon)$, integrating by parts with respect to time in the kinetic energy term, and making use of the initial and final conditions (5) and (6), we find

$$\frac{dS}{d\varepsilon} = -\int_0^T \int m(a)\frac{\partial^2 \mathbf{X}}{\partial t^2}(a, t, \varepsilon)\cdot\frac{\partial \mathbf{X}}{\partial \varepsilon}(a, t, \varepsilon)\, da\, dt$$
$$-\int_0^T \frac{d}{d\varepsilon}E[\mathbf{X}(\ , t, \varepsilon), t]\, dt. \tag{9}$$

Now apply Hamilton's principle and the definition of $\mathbf{f}$ (eq. (2)) to obtain

$$0 = \frac{dS}{d\varepsilon}(0) = \int_0^T \int \left[-m(a)\frac{\partial^2 \mathbf{X}}{\partial t^2}(a, t) + \mathbf{f}(a, t)\right]\cdot\frac{\partial \mathbf{X}}{\partial \varepsilon}(a, t, 0)\, da\, dt. \tag{10}$$

Equation (10) holds for all $\partial \mathbf{X}/\partial \varepsilon$ consistent with the constraints.

Before doing any further analysis of (10), we switch to Eulerian variables. Let $\mathbf{u}(\mathbf{x}, t)$ and $\mathbf{v}(\mathbf{x}, t)$ be implicitly defined by

$$\frac{\partial \mathbf{X}}{\partial t}(a, t) = \mathbf{u}(\mathbf{X}(a, t), t), \tag{11}$$

$$\frac{\partial \mathbf{X}}{\partial \varepsilon}(a, t, 0) = \mathbf{v}(\mathbf{X}(a, t), t). \tag{12}$$

In terms of $\mathbf{u}$ and $\mathbf{v}$, the constraint of volume conservation reduces to

$$\nabla\cdot\mathbf{u} = 0, \tag{13}$$

$$\nabla\cdot\mathbf{v} = 0. \tag{14}$$

These results can be derived by differentiating (8) with respect to t (to obtain $\nabla\cdot\mathbf{u} = 0$) or with respect to ε (to obtain $\nabla\cdot\mathbf{v} = 0$).

Differentiating (11) with respect to t, we obtain

$$\frac{\partial^2 \mathbf{X}}{\partial t^2}(a, t) = \left(\mathbf{u}\cdot\nabla\mathbf{u} + \frac{\partial \mathbf{u}}{\partial t}\right)(\mathbf{X}(a, t), t) = \frac{D\mathbf{u}}{Dt}(\mathbf{X}(a, t), t), \tag{15}$$

where we have introduced the shorthand $D\mathbf{u}/Dt$ for $\mathbf{u}\cdot\nabla\mathbf{u}+\partial\mathbf{u}/\partial t$. Despite its interpretation as the "material derivative" of the velocity, note that $D\mathbf{u}/Dt$ is a function of $(\mathbf{x}, t)$.

Additional functions of $(\mathbf{x}, t)$ that we shall need are mass density $\rho(\mathbf{x}, t)$ and the force density $\mathbf{F}(\mathbf{x}, t)$. These are defined as follows:

$$\rho(\mathbf{x}, t) = \int m(a)\delta(\mathbf{x} - \mathbf{X}(a, t))\, da, \tag{16}$$

$$\mathbf{F}(\mathbf{x}, t) = \int \mathbf{f}(a, t)\delta(\mathbf{x} - \mathbf{X}(a, t))\, da. \tag{17}$$

Making use of these definitions, we transform (10) to Eulerian form:

(18)

$$\begin{aligned} 0 &= \int_0^T \int \left[-m(a)\frac{\partial^2 \mathbf{X}}{\partial t^2}(a,t) + \mathbf{f}(a,t)\right] \cdot \frac{\partial \mathbf{X}}{\partial \varepsilon}(a,t,0)\, da\, dt \\ &= \int_0^T \int \int \left[-m(a)\frac{D\mathbf{u}}{Dt}(\mathbf{x},t) + \mathbf{f}(a,t)\right] \cdot \mathbf{v}(\mathbf{x},t)\delta(\mathbf{x} - \mathbf{X}(a,t))\, d\mathbf{x}\, da\, dt \\ &= \int_0^T \int \left[-\rho(\mathbf{x},t)\frac{D\mathbf{u}}{Dt}(\mathbf{x},t) + \mathbf{F}(\mathbf{x},t)\right] \cdot \mathbf{v}(\mathbf{x},t)\, d\mathbf{x}\, dt. \end{aligned}$$

To see that the second line of (18) is equivalent to the first, just apply the defining property of the Dirac δ-function, $\int \delta(\mathbf{x} - \mathbf{y})\phi(\mathbf{x})\, d\mathbf{x} = \phi(\mathbf{y})$. The third line follows by interchanging the order of integration and applying the definitions of ρ and $\mathbf{F}$, (16)–(17).

Now (18) holds for all $\mathbf{v}$ such that $\nabla \cdot \mathbf{v} = 0$. It follows that the coefficient of $\mathbf{v}$ must be the gradient of some quantity (which is conventionally called the pressure). This gives

$$\rho(\mathbf{x},t)\left(\frac{\partial \mathbf{u}}{\partial t} + \mathbf{u} \cdot \nabla \mathbf{u}\right) + \nabla p = \mathbf{F}(\mathbf{x},t). \tag{19}$$

Equation (19) may be augmented by the addition of a term that takes into account the presence of viscosity. (Frictional forces are not easily incorporated into the Lagrangian formalism used above.) For simplicity, we use a viscous force of the form $\mu\nabla^2\mathbf{u}$ with $\mu =$ constant. In the future one might want to modify this to allow for a different form or magnitude of the viscous force in the muscular heart walls or to model the non-Newtonian character of the blood. (The latter effect is a small one in vessels as large as the heart.)

We now summarize the equations of motion (with viscosity included). They are

$$\rho(\mathbf{x},t)\left(\frac{\partial \mathbf{u}}{\partial t} + \mathbf{u} \cdot \nabla \mathbf{u}\right) + \nabla p = \mu\nabla^2\mathbf{u} + \mathbf{F}(\mathbf{x},t), \tag{20}$$

$$\nabla \cdot \mathbf{u} = 0, \tag{21}$$

$$\rho(\mathbf{x},t) = \int m(a)\delta(\mathbf{x} - \mathbf{X}(a,t))\, da, \tag{22}$$

$$\mathbf{F}(\mathbf{x},t) = \int \mathbf{f}(a,t)\delta(\mathbf{x} - \mathbf{X}(a,t))\, da, \tag{23}$$

$$\frac{\partial \mathbf{X}}{\partial t}(a,t) = \mathbf{u}(\mathbf{X}(a,t),t) = \int \mathbf{u}(\mathbf{x},t)\delta(\mathbf{x} - \mathbf{X}(a,t))\, d\mathbf{x}, \tag{24}$$

$$\mathbf{f}(\,,t) = -E_{\mathbf{X}}[\mathbf{X}(\,,t),t], \tag{25}$$

where $E_{\mathbf{X}}$ denotes the Fréchet derivative of E with respect to $\mathbf{X}$ (see (2)).

Note that these equations may be partitioned naturally into three groups. The Eulerian group (20)–(21) may be recognized as the Navier-Stokes equations of a viscous incompressible fluid with variable mass density $\rho(\mathbf{x},t)$ and

an applied or external force density $\mathbf{F}(\mathbf{x}, t)$. In the present context, these equations are used not only for the blood in the cardiac chambers (where $\mathbf{F} \equiv 0$) but also for the muscular heart walls and the valves, where $\mathbf{F}$ is an expression of the elasticity of the material. The Lagrangian group contains only (25), which defines the elastic properties of the valve leaflets and the muscular heart walls. A more specific example will be given below. Finally, (22)–(24) may be described as interaction equations. They define certain Eulerian quantities in terms of Lagrangian quantities and vice versa. In each case, the interaction may be expressed as an integral transformation with a δ-function kernel.

It is easy to show from (22) and from volume conservation that $\rho(\mathbf{x}, t)$ is constant along particle trajectories: $\rho(\mathbf{X}(a, t), t) = m(a)/J_0(a)$. An important special case is where $m(a)/J_0(a) = \rho_0$, independent of a, for it then follows that $\rho(\mathbf{x}, t) = \rho_0$, independent of $\mathbf{x}$ and t. This special case is quite realistic for the heart, since cardiac muscle has nearly the same density as blood, and it is the only case for which we have actually implemented a scheme for the numerical solution of (20)–(25). The general case opens up an intriguing prospect of additional applications, however, in which a fluid interacts with an (active or passive) elastic medium of a different density. Bird flight is one example that comes to mind.

We conclude this section by discussing a special case of an elastic energy functional E that plays an important role in modeling the heart. A striking characteristic of cardiac muscle is that the heart is made of fibers and that there is a definite local fiber orientation that changes smoothly from point to point **[3–6]**. Let the Lagrangian parameters (q, r, s) be chosen in such a way that $q, r =$ constant along a fiber. We assume that E is of the form

$$E = \int \mathscr{E}\left(\left|\frac{\partial \mathbf{X}}{\partial s}\right|; q, r, s, t\right) dq\, dr\, ds; \tag{26}$$

that is, the local energy density depends only on the local fiber strain, which is determined by $|\partial \mathbf{X}/\partial s|$, and not on the strain in the cross-fiber directions. The Fréchet derivative of E is evaluated as follows:

(27)

$$\begin{aligned}\lim_{\varepsilon \to 0} \frac{d}{d\varepsilon} E[\mathbf{X} + \varepsilon \mathbf{Y}, t] &= \int \mathscr{E}'\left(\left|\frac{\partial \mathbf{X}}{\partial s}\right|; q, r, s, t\right) \frac{\partial \mathbf{X}/\partial s}{|\partial \mathbf{X}/\partial s|} \cdot \frac{\partial \mathbf{Y}}{\partial s}\, dq\, dr\, ds \\ &= -\int \frac{\partial}{\partial s}\left[\mathscr{E}'\left(\left|\frac{\partial \mathbf{X}}{\partial s}\right|; q, r, s, t\right) \frac{\partial \mathbf{X}/\partial s}{|\partial \mathbf{X}/\partial s|}\right] \cdot \mathbf{Y}\, dq\, dr\, ds.\end{aligned}$$

Here $\mathscr{E}'$ denotes the derivative of $\mathscr{E}$ with respect to its first argument. It follows (see (2)) that

$$\mathbf{f}(q, r, s, t) = \frac{\partial}{\partial s}(T\boldsymbol{\tau}), \tag{28}$$

where

$$T(q, r, s, t) = \mathscr{E}'\left(\left|\frac{\partial \mathbf{X}}{\partial s}\right| ; q, r, s, t\right), \tag{29}$$

$$\boldsymbol{\tau}(q, r, s, t) = \frac{\partial X/\partial s}{|\partial \mathbf{X}/\partial s|}. \tag{30}$$

The vector $\boldsymbol{\tau}$ is the unit tangent to the fibers, and the scalar T is the fiber tension in the sense that $T\boldsymbol{\tau}\, dq\, dr$ is the force transmitted by the bundle of fibers $dq\, dr$. Equations (28)–(30) may also be derived from more elementary force-balance arguments (see [7]).

The issue of numerical stability and the computation of the elastic force. The numerical method that we use to solve (20)–(25) in the special case that ρ is constant and that E is given by (26) is described in detail in [7–9]. Here we discuss only one aspect of this method (see also [10]): the influence of the particular way that $\mathbf{f}$ is computed on the stability of the computation as a whole. This issue arises because of the finite size of the time step Δt. Consider the step from $t = n\Delta t$ to $t = (n+1)\Delta t$. (We shall refer to this as time step n.) If the force used for this time step is computed according to the straightforward recipe $\mathbf{f} = -E_{\mathbf{X}}[\mathbf{X}(a, n\Delta t), n\Delta t]$, then the computed solution exhibits violent instability unless Δt is very small. The cause of this instability is that the fiber configurations may drastically overshoot equilibrium on a single time step. This results in a reversal of sign and a large increase in the magnitude of $\mathbf{f}$, a situation which compounds itself from one time step to the next.

One possible cure for this well-known "stiffness" difficulty is to compute the force that is used during time step n from the unknown fiber configuration $\mathbf{X}(a, (n+1)\Delta t)$. This "backward-Euler" or "implicit" approach has recently been tried (on a two-dimensional model problem in which the fluid is described by the Stokes equations) in the Ph.D. thesis of C. Tu [11a,b]. This work confirms the unconditional stability of the backward-Euler method, but it also makes clear the complexity of the dense nonlinear system that must then be solved for $\mathbf{f}$ at each time step.

Here, we describe an intermediate approach which enhances the stability of the method (without, unfortunately, making it unconditionally stable) at a more modest cost. (See [11a,b] for a comparison of all three methods.) The basic idea is to compute the force for time step n from a configuration that *approximates* $\mathbf{X}(a, (n+1)\Delta t)$. For this to work, however, it is crucial that the approximation include, at least crudely, the effect of $\mathbf{f}$ at time step n on $\mathbf{X}(a, (n+1)\Delta t)$. The approximation that we use is obtained by considering a model problem in which the Lagrangian is again given by (3) but the constraint of incompressibility (and the fluid viscosity) are ignored. The equations of motion for this model problem are simply

$$-m(a)\frac{\partial^2 \mathbf{X}}{\partial t^2}(a, t) + \mathbf{f}(a, t) = 0, \tag{31}$$

where

$$\mathbf{f}(\ ,t) = -E_{\mathbf{X}}[\mathbf{X}(\ ,t),t] \tag{32}$$

as before. Equation (31) may be put in first-order form by introducing $\mathbf{U}(a,t) = (\partial\mathbf{X}/\partial t)(a,t) = \mathbf{u}(\mathbf{X}(a,t),t)$. Then

$$-m(a)\frac{\partial \mathbf{U}}{\partial t}(a,t) + \mathbf{f}(a,t) = 0, \tag{33}$$

$$\frac{\partial \mathbf{X}}{\partial t}(a,t) = \mathbf{U}(a,t). \tag{34}$$

Now the backward-Euler method for the system comprised of (32)–(34) is as follows:

$$-m(a)\frac{\mathbf{U}^{n+1}(a) - \mathbf{U}^n(a)}{\Delta t} + \mathbf{f}^{n+1}(a) = 0, \tag{35}$$

$$\frac{\mathbf{X}^{n+1}(a) - X^n(a)}{\Delta t} = \mathbf{U}^{n+1}(a), \tag{36}$$

$$\mathbf{f}^{n+1}(\ ) = -E_{\mathbf{X}}^{n+1}[\mathbf{X}^{n+1}(\ )], \tag{37}$$

where the superscripts denote the time step index, as in $\mathbf{X}^n(a) = \mathbf{X}(a, n\Delta t)$.

We now derive an energy inequality for the difference equations (35)–(37) which gives some insight into the good stability properties of the backward-Euler method. The inequality is derived under the hypothesis that E^n is a *convex* functional for every n. This means that

$$E^n[\mathbf{Y}] \geq E^n[\mathbf{X}] + (\mathbf{Y} - \mathbf{X}, E_{\mathbf{X}}^n[\mathbf{X}]), \tag{38}$$

where $(\ ,\ )$ denotes the inner product

$$(\mathbf{X}, \mathbf{Y}) = \int \mathbf{X}(a)\cdot\mathbf{Y}(a)\,da. \tag{39}$$

(We leave it as an exercise for the reader to show that the particular energy functional given by (26) is convex provided that $\mathscr{E}' \geq 0$, $\mathscr{E}'' \geq 0$, $\mathscr{E}'(0;q,r,s,t) = \mathscr{E}''(0;q,r,s,t) = 0$.) We apply the foregoing definition of convexity to (35)–(37) in the following way:

$$\begin{aligned} E^{n+1}[\mathbf{X}^n] &\geq E^{n+1}[\mathbf{X}^{n+1}] + (\mathbf{X}^n - \mathbf{X}^{n+1}, E_{\mathbf{X}}^{n+1}[\mathbf{X}^{n+1}]) \\ &= E^{n+1}[\mathbf{X}^{n+1}] + \Delta t(\mathbf{U}^{n+1}, \mathbf{f}^{n+1}) \\ &= E^{n+1}[\mathbf{X}^{n+1}] + (\mathbf{U}^{n+1}, m(\mathbf{U}^{n+1} - \mathbf{U}^n)) \\ &= E^{n+1}[\mathbf{X}^{n+1}] + \tfrac{1}{2}(\mathbf{U}^{n+1}, m\mathbf{U}^{n+1}) - \tfrac{1}{2}(\mathbf{U}^n, m\mathbf{U}^n) \\ &\quad + \tfrac{1}{2}((\mathbf{U}^{n+1} - \mathbf{U}^n), m(\mathbf{U}^{n+1} - \mathbf{U}^n)). \end{aligned} \tag{40}$$

Because the last term is positive, we may throw it away without disturbing the inequality. Rearranging the result and writing $E^{n+1}[\mathbf{X}^n] = E^n[\mathbf{X}^n] + (E^{n+1} - E^n)[\mathbf{X}^n]$, we get

$$E^{n+1}[\mathbf{X}^{n+1}] + \tfrac{1}{2}(\mathbf{U}^{n+1}, m\mathbf{U}^{n+1}) \leq E^n[\mathbf{X}^n] + \tfrac{1}{2}(\mathbf{U}^n, m\mathbf{U}^n) + (E^{n+1} - E^n)[\mathbf{X}^n]. \tag{41}$$

For a time-independent elastic energy functional (E^n independent of n), the inequality that we have just derived states that the total energy at time $t = (n+1)\Delta t$ is bounded by the total energy at $t = n\Delta t$ and hence by the total energy at $t = 0$. In the general case, the inequality states that the increase in the total energy at time step n is at most the increase in elastic energy that would have occurred if the system had been artificially held at $\mathbf{X}^n$. These reasonable bounds prevent the explosive growth in energy that may occur when $\mathbf{f}^n$ is used in place of $\mathbf{f}^{n+1}$ in (35).

Let us now consider the practical question of how to solve (35)–(37) for the unknowns $\mathbf{X}^{n+1}$, $\mathbf{U}^{n+1}$, $\mathbf{f}^{n+1}$. Eliminating $\mathbf{U}^{n+1}$ and $\mathbf{f}^{n+1}$, we find

$$m(\mathbf{X}^{n+1} - \mathbf{X}^{n+1,0}) + (\Delta t)^2 E_{\mathbf{X}}^{n+1}[\mathbf{X}^{n+1}] = 0, \tag{42}$$

where

$$\mathbf{X}^{n+1,0} = \mathbf{X}^n + \Delta t \mathbf{U}^n. \tag{43}$$

Note that (42) is of the form

$$\phi_{\mathbf{X}}^{n+1}[\mathbf{X}^{n+1}] = 0, \tag{44}$$

where $\phi_{\mathbf{X}}^{n+1}$ is the Fréchet derivative of the functional ϕ^{n+1} defined by

$$\phi^{n+1}[\mathbf{X}] = \tfrac{1}{2}(\mathbf{X} - \mathbf{X}^{n+1,0}, m(\mathbf{X} - \mathbf{X}^{n+1,0})) + (\Delta t)^2 E^{n+1}[\mathbf{X}]. \tag{45}$$

Thus, the solutions of (42) are the stationary points of ϕ^{n+1}. Among the different types of stationary points that one might consider, it is intuitively clear that minima are best from the standpoint of stability. Moreover, ϕ^{n+1} is guaranteed to have at least one minimum provided that $m(a)$ is bounded from below by some positive constant m_0, that E^{n+1} is bounded from below (say) by zero, and that E^{n+1} is continuous. Thus, one may use any algorithm that searches for a local minimum of ϕ^{n+1} to find a solution $\mathbf{X}^{n+1}$ of (42). We use algorithms based on Newton's method for this task.

Of course, the scheme given by (35)–(37) solves only the model problem in which incompressibility and viscosity are ignored. How can we use it in the solution of the full system (20)–(25)? What we actually do is described as follows. At each time step, we begin by solving difference equations of the same form as (35)–(37) but with the unknowns $\mathbf{X}^{n+1}$, $\mathbf{U}^{n+1}$, $\mathbf{f}^{n+1}$ replaced by $\mathbf{X}^{n+1,*}$, $\mathbf{U}^{n+1,*}$, $\mathbf{f}^{n+1,*}$, the notation being changed because these quantities no longer have the status of being the final results of the time step. No further use is made of $\mathbf{X}^{n+1,*}$ or $\mathbf{U}^{n+1,*}$, but the force $\mathbf{f}^{n+1,*}$ is then used as input to the algorithm that updates the solution of (20)–(24). For details of this algorithm, see [7].

The method of computing $\mathbf{f}$ that we have just described differs from our previously published work by the inclusion of the nonconstant factor $m(a)$. In certain problems $m(a)$ may be given, but in others it may have to be estimated from the given mass density of the material and the spatial distribution of the Lagrangian marker points.

To discuss the latter situation, we must say a little about the spatial discretization of the equations. The Eulerian variable $\mathbf{x}$ is represented by a regular cubic lattice of points $\mathbf{x}_\mathbf{j} = \mathbf{j}h$, where h is the lattice spacing. The Lagrangian parameter a is represented by some finite collection of values a_k each with an associated "volume" in parameter space Δa. We let $m_k = m(a_k)$ and $\mathbf{X}_k^n = \mathbf{X}(a_k, n\Delta t)$. The product $m_k \Delta a$ is the mass associated with material element k. Note that the points $\mathbf{X}_k^n$ need not coincide with any of the lattice points $\mathbf{x}_\mathbf{j}$. The connection between the discrete Lagrangian and Eulerian representations is made with the help of a spread-out version of the δ-function, which we denote δ_h. For the specific definition of δ_h and for a discussion of its properties, see [**12**, 13]. This function is used in the discretization of the interaction equations (22)–(24).

We now turn to the task of estimating m_k in cases where $m(a)$ is not given. Suppose, for example, that $\rho(\mathbf{x}, t) = \rho_0$ as in the heart problem. Evaluating this at $\mathbf{x} = \mathbf{X}(a, t)$ we get

$$\begin{aligned} \rho_0 &= \rho(\mathbf{X}(a,t),t) = \int \rho(\mathbf{x},t)\delta(\mathbf{x}-\mathbf{X}(a,t))\,d\mathbf{x} \\ &= \iint m(a')\delta(\mathbf{x}-\mathbf{X}(a',t))\delta(\mathbf{x}-\mathbf{X}(a,t))\,d\mathbf{x}\,da', \end{aligned} \tag{46}$$

where we have used the definition of the δ-function and also (16), which defines ρ in terms of m. Clearly we may replace $m(a')$ by $m(a)$ in (46). [To see this, do the $\mathbf{x}$ integral first to obtain $\rho_0 = \int m(a')\delta(\mathbf{X}(a',t)-\mathbf{X}(a,t))\,da'$ and use the invertibility of $\mathbf{X}(\ ,t)$.] Thus we may write

$$m(a) = \frac{\rho_0}{\iint \delta(\mathbf{x}-\mathbf{X}(a',t))\delta(\mathbf{x}-\mathbf{X}(a,t))\,d\mathbf{x}\,da'}. \tag{47}$$

This is equivalent to $m(a) = \rho_0 J_0(a)$, but (47) is more useful for our purpose, which is to estimate $m(a)$ solely from the given distribution of Lagrangian markers at any particular time. To do this, we discretize (47) as follows:

$$m_k = \frac{\rho_0}{\sum_l \sum_\mathbf{j} \delta_h(\mathbf{x}_\mathbf{j}-\mathbf{X}_l)\delta_h(\mathbf{x}_\mathbf{j}-\mathbf{X}_k)h^3\Delta a} \tag{48}$$

or

$$m_k \Delta a = \frac{\rho_0}{\sum_l A_{kl}}, \tag{49}$$

where

$$A_{kl} = \sum_\mathbf{j} \delta_h(\mathbf{x}_\mathbf{j}-\mathbf{X}_l)\delta_h(\mathbf{x}_\mathbf{j}-\mathbf{X}_k)h^3. \tag{50}$$

The formula for m_k that we have just derived is new. In previous work [7, 8, 10–13, 17–19] we used the approximation to (49) given by

$$m_k \Delta a \approx \frac{\rho_0}{A_{kk}} = \left(\frac{8}{3}\right)^3 \rho_0 h^3, \tag{51}$$

which seemed reasonable because our particular choice of δ_h is such that $0 \leq A_{kl} \leq A_{kk} = (\frac{3}{8h})^3$ and because most of the off-diagonal terms of A are zero. In fact, (49) reduces to (51) when the Lagrangian markers are so far apart that the support of their δ_h-functions do not overlap. We were forced to reconsider the use of this approximation, however, when we constructed a heart model in which large numbers of Lagrangian markers were crowded close together in a particular plane, which is the plane of valve rings. A violent instability then appeared which was confined to the plane of the rings and which gave a strong visual hint that the high local density of Lagrangian markers was the culprit. This instability disappeared when we replaced (51) by (49). Intuitively, this is because (49) takes account of the high local number density of Lagrangian markers and assigns an appropriately small mass to each of them.

Applications (cardiac fluid dynamics). A two-dimensional version of the above-described computational method has been used in a series of studies concerning the mitral valve, which is the inflow valve to the left ventricle of the heart. Some of these studies have involved the natural mitral valve, while others have been aimed at the improved design of mechanical valves for the replacement of diseased mitral valves.

In the case of the natural mitral valve, the computational method has been used to confirm and refine Leonardo da Vinci's theory [**14**] concerning the role of the valve-generated vorticity in efficient valve closure [**12**, 15]. It has also been used to determine the optimal time delay between the contraction of the atrium and that of the ventricle [**16**]. Simulation of a disease process (prolapse of the mitral valve) has been achieved by adjusting the parameters of the model heart [**17**].

Parametric studies aimed at optimizing the design of prosthetic mitral valves have also been performed. In particular, the optimal pivot point and curvature have been determined for pivoting single-disc valves [**18**] and for butterfly leaflet valves [**19**]. The design criteria used in these studies are intended to create valves with good pressure-flow characteristics and with a low propensity for stagnation and thrombosis.

Our recent efforts have been dedicated to the three-dimensional implementation of the computational method [**7–9**] and to the construction of a three-dimensional fiber-based computer model of the heart for use with that method. The method is operational, and the model is near completion. Some preliminary results are shown in Figure 1.

The equations of Newtonian molecular dynamics. The goal of molecular dynamics is to describe the motion of a single molecule (or of a collection of molecules) at the *atomic* level of description. Thus, the dynamical variables are the coordinates and momenta of the atoms; there is no attempt to look inside the atoms at their electronic (or nuclear) structure. Note that

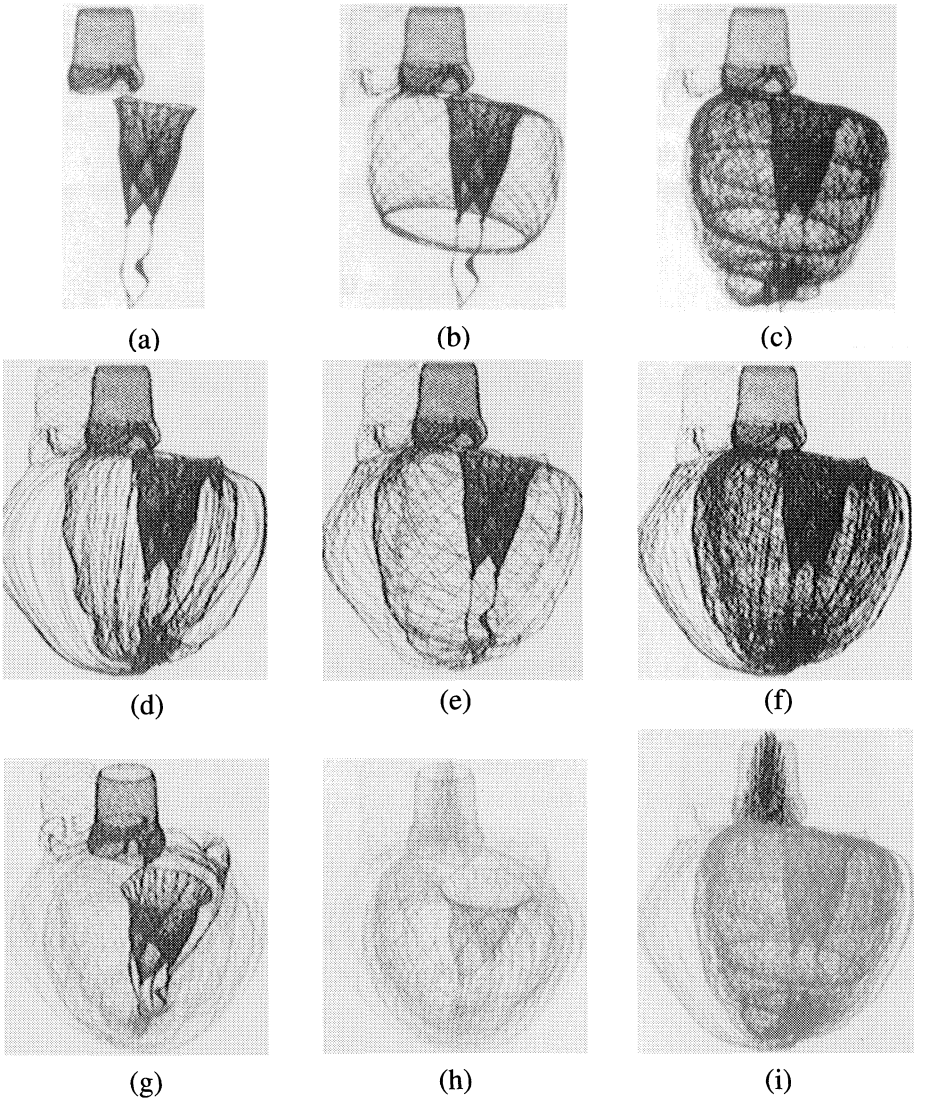

FIGURE 1. A computer model of the heart at a single instant during ventricular ejection.

(a) Detail of the mitral and aortic valves.
(b) The pulmonic valve and a (double-sheeted) layer of the left ventricular wall have been added.
(c) Additional layers of the left ventricular wall. Each layer is double-sheeted with the fibers making a smooth transition from one sheet to the other at their common edge. The different layers are nested.
(d) Vertical fibers that surround the heart as a whole, penetrate at the apex, and form the inner lining of the left ventricle. Note the right ventricle (left in figure). The tricuspid valve is obscured by the mitral valve in this view.
(e) A layer of fibers that wraps (figure-eight fashion) around both ventricles.
(f) Complete model of the left and right ventricles connected to the aorta and the pulmonary artery.
(g) A perspective view of the complete model with all four valves visible.
(h) Velocity vectors emanating from the plane of the aortic valve ring (viewpoint from slightly above the plane).
(i) The same velocity vectors viewed from within the plane of the aortic valve ring.

the atomic level is perhaps the smallest at which it makes sense to think in classical (as opposed to quantum-mechanical) terms. Even here, however, there are certain quantum effects that should not be ignored. An important theme of the work that we shall describe is how to include such effects in an essentially classical description.

The classical equations of motion of a molecular system may be written in the form

$$M\frac{d^2X}{dt^2} + E'(X) = 0, \tag{52}$$

where X is a vector with $N = 3n_a$ components ($n_a = \#$ of atoms) that lists the Cartesian coordinates of the atoms, M is a diagonal matrix of order $3n_a$ with diagonal entries equal to the masses of the atoms (each mass repeated three times), $E(X)$ is the potential energy of the molecular system as a function of its configuration X, and E' denotes the gradient of E.

The mass matrix M and the potential energy function E define the system. In principle (according to the Born-Oppenheimer approximation [**20**]), the value of E at each configuration X may be found by solving the Schrödinger equation of the electrons with the atomic nucleic held fixed in the configuration X. In practice, the function $E(X)$ is obtained by a much less systematic procedure that combines guesswork, empirical data, and theoretical considerations. In this "empirical" approach, there are two types of terms that appear in $E(X)$: bonded and nonbonded. In the first category are energies associated with bond stretching, with distortions in bond angle, and with rotations about individual bonds. In the second category are the Coulomb and Van der Waals energies; these involve sums over all atom pairs.

A typical energy function is constructed as follows. Let the atoms be numbered $i = 1, \ldots, n_a$, and let $B_{ij} = 1$ if $i \neq j$ and there is a chemical bond connecting atom i to atom j, with $B_{ij} = 0$ otherwise. Then let

$$S_2 = \{(i, j) : B_{ij} = 1\}, \tag{53}$$

$$S_3 = \{(i, j, k) : (i, j) \in S_2, (j, k) \in S_2, i \neq k\}, \tag{54}$$

$$S_4 = \{(i, j, k, l) : (i, j, k) \in S_3, (j, k, l) \in S_3\}. \tag{55}$$

In the foregoing definitions, (i, j), (i, j, k), and (i, j, k, l) denote *ordered* pairs, triples, and quadruples of integers selected from $\{1, \ldots, n_a\}$. Also let

$$\mathbf{X}_{ij} = \mathbf{X}_j - \mathbf{X}_i, \tag{56}$$

$$\mathbf{X}_{ijk} = \mathbf{X}_{ij} \times \mathbf{X}_{jk}, \tag{57}$$

and introduce the notation $\theta(\mathbf{a}, \mathbf{b})$ for the angle between the two vectors $\mathbf{a}$ and $\mathbf{b}$. (That is, $\cos\theta(\mathbf{a}, \mathbf{b}) = (\mathbf{a} \cdot \mathbf{b})/(|\mathbf{a}|\,|\mathbf{b}|)$ and $0 \leq \theta(\mathbf{a}, \mathbf{b}) \leq \pi$.)

For $(i, j) \in S_2$, $|\mathbf{X}_{ij}|$ is the length of the bond connecting atom i and atom j. For $(i, j, k) \in S_3$, $\theta(\mathbf{X}_{ji}, \mathbf{X}_{jk})$ is a bond angle with vertex at atom

j. For $(i, j, k, l) \in S_4$, $\theta(\mathbf{X}_{ijk}, \mathbf{X}_{jkl})$ is the dihedral angle about the bond connecting atom j and atom k.

With the notation introduced above, the potential energy E of the molecular system may be defined as follows:

$$
\begin{aligned}
2E(\mathbf{X}_1 \cdot s\mathbf{X}_{n_a}) = & \sum_{(i,j)\in S_2} f_{ij}(|\mathbf{X}_{ij}|) + \sum_{(i,j,k)\in S_3} f_{ijk}(\theta(\mathbf{X}_{ji}, \mathbf{X}_{jk})) \\
& + \sum_{(i,j,k,l)\in S_4} f_{ijkl}(\theta(\mathbf{X}_{ijk}, \mathbf{X}_{jkl})) \\
& + \sum_{(i,j):\, i\neq j} \left\{ \frac{q_i q_j}{4\pi\varepsilon|\mathbf{X}_{ij}|} + \left(\frac{a_{ij}}{|\mathbf{X}_{ij}|^{12}} - \frac{b_{ij}}{|\mathbf{X}_{ij}|^{6}} \right) \right\}.
\end{aligned} \tag{58}
$$

The factor 2 on the left-hand side of (58) reflects the fact that each term on the right appears exactly twice. If $(i, j, k) \in S_3$, for example, then $(k, j, i) \in S_3$, the functions f_{ijk} and f_{kji} are the same, and $\theta(\mathbf{X}_{ji}, \mathbf{X}_{jk}) = \theta(\mathbf{X}_{jk}, \mathbf{X}_{ji})$. The functions f_{ij}, f_{ijk}, and f_{ijkl} which appear in (58) specify respectively the energies associated with bond length, bond angle, and dihedral angle. One might, for example, set $f_{ij}(r) = \frac{1}{2}K_{ij}(r - (r_0)_{ij})^2$, where the parameters K_{ij} and $(r_0)_{ij}$ would be determined by the atom types (C, O, N, H, $\cdot s$) of the two atoms i and j and by the type of bond (single, double, aromatic, ...) that connects these two atoms. The last summation in (58) describes the nonbonded interactions. In these terms the q_i are the partial charges, ε is the dielectric constant (see below), and the coefficients a_{ij}, b_{ij} describe the Van der Waals interaction between atoms i and j. (These coefficients are determined by the atom types of the two atoms in question.) The appropriate dielectric constant is that of free space if all atoms in the system are modeled explicitly. Otherwise it may be necessary to adjust the dielectric constant to account for the screening effect of charges or dipoles that are not explicitly modeled.

The backward-Euler Langevin method. For systems with large numbers of atoms, the numerical solution of (52) is plagued by the same "stiffness" difficulty that arises in the case of cardiac fluid dynamics, as described above. Here we see the problem in its pure form without the complications introduced by the fluid. In fact, the molecular dynamics problem is of precisely the same form as the model problem that was used for the computation of the elastic force in the cardiac case (see (31)–(32)).

In the molecular case, however, the wide disparity of time scales that is the fundamental source of the stiffness difficulty mentioned above has additional physical significance. The fastest time scales in the classical problem are not only awkward to compute, they are actually filtered out by quantum-mechanical effects. This is because a mode with natural frequency ω has a high probability of being found in its ground state when $\hbar\omega > kT$, where $\hbar$ is Planck's constant divided by 2π, k is Boltzmann's constant, and T is

the temperature. This has the important consequence of limiting the number of modes that contribute to the specific heat of a substance at any given temperature [**21**]. Thus, a purely classical computation will overestimate the specific heat, sometimes drastically.

These considerations suggest the use of the backward-Euler method for the numerical solution of (52), both because that method makes possible stable computations with large time steps and also because it filters out high-frequency modes in a way that is reminiscent of the filtering provided by quantum mechanics. A fundamental difficulty that immediately comes to mind, however, is the dissipative character of the backward-Euler method as expressed, for example, by the energy inequality (41). A computational method in which the energy continually runs down does not seem to be a reasonable model of a molecular system at a given temperature. The way out of this difficulty is to excite the system continually with a random force that simulates the interaction with a thermal reservoir. This makes it possible to establish and maintain a prescribed temperature T despite the dissipation introduced by the backward-Euler method. We call this combination the "backward-Euler/Langevin method," since it amounts to a backward-Euler discretization of the Langevin equations of motion.

An important feature of the backward-Euler/Langevin method is the choice of parameters. The particular choice that we shall describe results in a cutoff frequency ω_c that is independent of the time step Δt (provided that $\omega_c \Delta t$ is small). By setting $\omega_c = kT/\hbar$, one can simulate (in an otherwise classical context) the quantum-mechanical suppression of high-frequency molecular motions.

The classical Langevin equations of motion are a modification of (52) that is obtained by imposing both a random force and a frictional force as follows:

$$M\left(\frac{d^2X}{dt^2} + \gamma\frac{dX}{dt}\right) + E'(X) = R(t). \tag{59}$$

Here γ is a parameter with units of reciprocal time that is called the "collision frequency," and $R(t)$ is a vector-valued stationary stochastic process with the following first and second moments:

$$\langle R(t)\rangle = 0, \tag{60}$$

$$\langle R(t)(R(t'))^{\mathrm{T}}\rangle = 2kT\gamma\delta(t-t')M. \tag{61}$$

Here $\langle\ \rangle$ denotes the ensemble average and the superscript $^{\mathrm{T}}$ denotes the transpose of a matrix. (We regard R as a column vector, so R^{T} is a row vector.) Note the appearance of the collision frequency γ not only as coefficient of the friction term in (59) but also in the covariance of the random force, (62).

Discretizing the foregoing equations according to the backward-Euler method, we obtain the discrete-time stationary stochastic process that is im-

plicitly defined as

$$(1+\gamma\Delta t)M(X^{n+1}-X^{n+1,0})+(\Delta t)^2E'(X^{n+1})=0, \tag{62}$$

where

$$X^{n+1,0}=X^n+\frac{(X^n-X^{n-1})+(\Delta t)^2M^{-1}R^{n+1}}{1+\gamma\Delta t}, \tag{63}$$

$$\langle R^n\rangle=0, \tag{64}$$

$$\langle R^n(R^{n'})^{\mathrm{T}}\rangle=2kT\gamma\frac{\delta_{nn'}}{\Delta t}M. \tag{65}$$

As in the cardiac case, one can compute X^{n+1} by minimizing the function

$$\phi^{n+1}(X)=\tfrac{1}{2}(X-X^{n+1,0})^{\mathrm{T}}M(X-X^{n+1,0})+(\Delta t)^2E(X). \tag{66}$$

A reasonable initial guess for this minimization is $X^{n+1,0}$. Equations (62)–(65) define the backward-Euler/Langevin method [22–24].

The choice of parameters. The computational method that we have just described has three adjustable parameters: T, γ, and Δt. It turns out that the ratio $\gamma/\Delta t$ is an important quantity which we shall call ω_c^2. We have studied the continuum limit of the backward-Euler/Langevin method as $\Delta t\to 0$ with ω_c fixed [22, 24]. Note that this limit is *not* described by the continuous Langevin equations of motion, since $\gamma\to 0$ along with Δt. In the special case of a system of coupled harmonic oscillators with frequencies ω_j, we have shown that the mean energy of the system is given (in the above-described limit) by

$$\langle E\rangle=\sum_j\frac{kT}{1+(\omega_j/\omega_c)^2}. \tag{67}$$

According to (67), the modes for which $\omega_j\ll\omega_c$ each contribute nearly kT to the total mean energy. Such modes, then, behave as in the classical statistical mechanics of a system at temperature T; this substantiates the interpretation of the parameter T as the temperature of the system, at least for the low-frequency modes. The modes for which $\omega_j\gg\omega_c$, on the other hand, each contribute $\ll kT$ to the total mean energy. Since the transition between the two regimes occurs near ω_c, we refer to ω_c as the *cutoff* frequency. We call these modes for which $\omega_j<\omega_c$ the *active* modes and those for which $\omega_j>\omega_c$ the *inactive* modes.

In practice one cannot set $\Delta t=0$, but to resolve all of the active modes it is only necessary to pick Δt so that $\omega_c\Delta t\ll 1$. There is no point in resolving the inactive modes, since they are repressed in any case. Depending on the choice of ω_c, the restriction $\omega_c\Delta t\ll 1$ may be much less severe than the restriction $(\max\{\omega_j\})\Delta t\ll 1$, which would have to be imposed for stability reasons if an explicit scheme were used.

In summary, the parameters should be selected as follows. First, set T equal to the (absolute) temperature of interest. Next, choose a cutoff frequency ω_c that marks the upper limit of the frequency range of interest. Finally select Δt so that $\Delta t\omega_c \ll 1$, and set $\gamma = \omega_c^2 \Delta t$.

We conclude this section with a qualitative discussion of what happens as the parameter Δt is varied within the limits implied by the restriction $\Delta t\omega_c \ll 1$. If Δt is made smaller, γ also becomes smaller, since $\gamma = \omega_c^2 \Delta t$. The effect of this is to reduce the influence of both the friction term and the random force on the backward-Euler/Langevin process. This is evident for the friction term but less so for the random force, since the covariance of the random force has amplitude $\gamma/\Delta t = \omega_c^2$, independent of Δt. Nevertheless, the continuum limit of a discrete-time random process with first and second moments given by $\langle r^n \rangle = 0$ and $\langle r^n r^m \rangle = \delta_{nm}$ is the zero process. The reason is that there is so much opportunity for cancellation as $\Delta t \to 0$. In summary, a reduction in Δt weakens the Langevin terms that provide coupling between the molecular system and the thermal reservoir which establishes and maintains the target temperature T. This has no effect on the equilibrium properties of the system, but it does reduce the rate at which such equilibrium is achieved, and it also increases the duration of a system trajectory that one must examine in order to obtain reliable estimates of equilibrium quantities. If Δt is reduced by a factor of 2, twice as much time (and hence a record containing *four* times as many time steps) is required to obtain averages with the same reliability as before.

A connection with quantum statistical mechanics. The suppression of fast modes that occurs in the backward-Euler/Langevin method is reminiscent of a similar suppression that occurs in quantum statistical mechanics. This physical effect plays an important role in the specific heat of diatomic gases, for example. At high temperature (e.g., 3000°K) such gases have a mean internal energy of $\frac{7}{2}kT$ per molecule. This is as predicted by classical statistical mechanics (provided that we regard the molecule as two point masses connected by a spring and ignore the electronic degrees of freedom!) The factor 7 is arrived at by counting three translational and two rotational degrees of freedom together with one vibrational degree of freedom (which counts twice because of the kinetic and potential vibrational energies). As the temperature is lowered, however, a new phenomenon appears which is completely inexplicable from a classical point of view [21]. First, the vibrational energy drops out of the picture and the molecule acts like two point masses connected by a rigid rod: its mean internal energy in this regime is $\frac{5}{2}kT$. This is the typical situation near room temperature. At still lower temperature (e.g., $30°K$) the rotation also drops out and the molecule acts like a monatomic gas: its mean internal energy is then only $\frac{3}{2}kT$.

These effects are important not only because they influence the mean energy that a molecule will carry at any given temperature, but also because they

imply that the real motions of the atoms in a complex molecule at ordinary temperatures are much more highly *correlated* than one would expect on the basis of classical statistical mechanics. This simplifying feature should be exploited in molecular dynamics computations.

The analogy between the suppression of fast modes in quantum statistical mechanics and the corresponding suppression in the backward-Euler/Langevin method can be made somewhat quantitative by making a particular choice of the cutoff frequency: $\omega_c = kT/\hbar$. We call this the quantum-mechanical cutoff frequency. With this choice the formula for the mean energy of a collection of coupled harmonic oscillators modeled by backward-Euler/Langevin method (equation (67)) becomes

$$\langle E\rangle_{\mathrm{BEL}} = \sum_j \frac{kT}{1+(\hbar\omega_j/kT)^2} \tag{68}$$

(in which the subscript BEL denotes backward-Euler/Langevin). This should be compared with the quantum-mechanical formula derived by Planck [25]

$$\langle E\rangle_{\mathrm{QM}} = \sum_j = \frac{kT(\hbar\omega_j/kT)}{\exp(\hbar\omega_j/kT)-1} \tag{69}$$

(where QM denotes quantum-mechanical). Note that (69) does not include the zero-point energy $\sum_j \frac{1}{2}(\hbar\omega_j)$ which would be present even at absolute zero temperature. Thus, (69) gives the energy required to raise the temperature of the system of coupled harmonic oscillators from absolute zero to the temperature T. It is also of interest to compare $\langle E\rangle_{\mathrm{BEL}}$ with the classical expression for the mean energy of a system of coupled harmonic oscillators. The classical result is

$$\langle E\rangle_{\mathrm{CM}} = \sum_j (kT) \tag{70}$$

(in which CM denotes classical mechanics). This formula is easily derived from (69) (or for that matter from (68)) by letting $\hbar \to 0$.

The three formulas given by (68)–(70) are all of the form

$$\langle E\rangle = \sum_j kT f\left(\frac{\hbar\omega_j}{kT}\right), \tag{71}$$

but the function f is different in each case:

$$f_{\mathrm{BEL}}(\theta) = \frac{1}{1+\theta^2}, \tag{72}$$

$$f_{\mathrm{QM}}(\theta) = \frac{\theta}{\exp(\theta)-1}, \tag{73}$$

$$f_{\mathrm{CM}}(\theta) = 1. \tag{74}$$

These three functions are plotted in Figure 2 (on the next page). Note the close resemblance of f_{BEL} and f_{QM} and also strong disagreement between

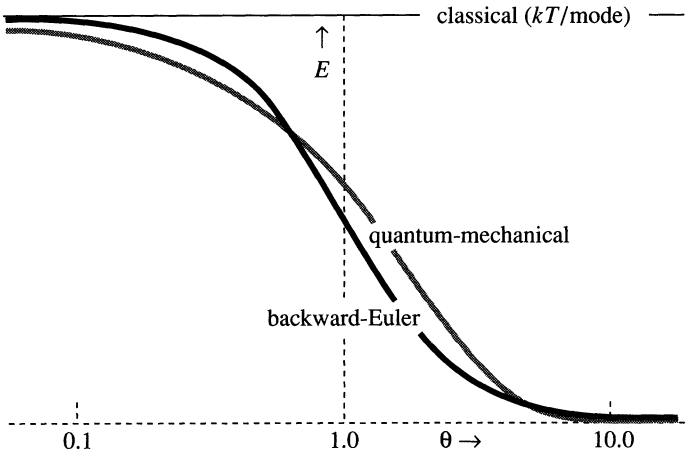

FIGURE 2. Comparison of thebackward-Euler/Langevin method with classical mechanics and with quantum mechanics. All three graphs refer to a coupled system of harmonic oscillators at temperature T. The ordinate E is the mean energy per vibrational mode, and the abscissa θ is the scaled natural frequency of the mode in question ($\theta = \hbar\omega/kT$) plotted on a logarithmic scale. In the classical case the mean energy is the same for all modes, while in both the quantum case and in the backward-Euler/Langevin case the mean energy per mode decreases dramatically as ω crosses the frequency given by $kT/\hbar$. For further details, see [22].

f_{BEL} and f_{CM}. This is quite astonishing when one considers the classical character of the backward-Euler/Langevin method.

Of course, the harmonic-oscillator problem is very special, and so one should consider other (nonlinear) examples. This has been done computationally for a diatomic molecule with bond energy given by a Morse potential [23]. As in quantum statistical mechanics, the specific heat computed by the backward-Euler/Langevin method is roughly $\frac{5}{2}k$ at moderate temperature and rises to $\frac{7}{2}k$ at high temperatures. The transition occurs as the vibrational motion comes into play. (Computations were not performed at low enough temperatures to see the $\frac{3}{2}k$ specific heat that should be observed when both vibration and rotation are inactive, but this was remedied in the analytic study of a rigid rotator, described below.)

In addition to this computational study of a diatomic molecule, we have also worked out an analytic framework for studying the equilibrium properties of a general Hamiltonian system modeled by the backward-Euler/

Langevin method [24]. This framework has been applied to the case of a rigid rotator, for which we have again obtained results which are qualitatively consistent with quantum statistical mechanics (though the agreement is less good than in the harmonic-oscillator case) and qualitatively *in*consistent with classical statistical mechanics.

Applications (molecular dynamics). The principal application of the backward-Euler/Langevin method will be the computational prediction of the three-dimensional structure of large biological molecules such as proteins and nucleic acids. (For an overview of this field, see [26].) A dynamic method is needed for this apparently static problem for the following reason. Large biological molecules have energy functions with multiple local minima. For a complete description of molecular structure it is not sufficient to find the global minimum (even if one knew how to do so). Rather, one needs to construct a catalog of low-energy minima, to determine the fraction of time that the molecule spends near each of them, and to evaluate the rate constants for the spontaneous transitions from one local minimum to another. The most straightforward way to collect this information is to simulate the physical process by which the molecule changes its configuration over time and to compile statistics concerning the molecular trajectory in configuration space. For such statistics to be meaningful, it is necessary that the simulated trajectory be of long enough duration to be representative. It is our hope that the backward-Euler/Langevin method will make this possible. For preliminary results, see [22, 27].

Conclusions. Hearts and biological macromolecules have more in common than might at first appear. Each can be viewed as an elastic structure, the dynamics of which is governed by an internal energy function. Each has many degrees of freedom and is capable of motions on widely different temporal (and spatial) scales. These multiple time scales require the use of implicit numerical methods, which can be formulated as optimization problems to be solved at each time step.

These similarities notwithstanding, there are also important differences between the two problems. In the cardiac case, the elastic energy function is time-dependent, and the elastic structure interacts with a viscous, incompressible fluid. In the molecular case, thermal fluctuations are important and quantum effects cannot be ignored.

As the present paper has shown, one can exploit the similarities between the two problems without overlooking the differences. This is done by using a common computational framework based on the backward-Euler method. In the cardiac case, however, this framework is coupled to the numerical solution of the Navier-Stokes equations, while in the molecular case, random forces are used to simulate thermal collisions, and parameters are chosen so that the backward-Euler dissipation simulates the quantum-mechanical suppression of fast molecular motions.

Acknowledgment. The cardiac research described in this paper is joint work with David M. McQueen; it is supported by the National Institutes of Health under research grant HL17859. The molecular-dynamics research is joint work with Tamar Schlick; it is supported by the National Science Foundation under research grant ASC8705589. The author is indebted to the mathematical community for providing a warm and supportive home for this interdisciplinary research.

REFERENCES

1. D. G. Ebin and R. A. Saxton, *The initial-value problem for elastodynamics of incompressible bodies*, Arch. Rational Mech. Anal. **94** (1986), 15–38.
2. ——, *The equations of incompressible elasticity*, Contemp. Math. **60** (1987), 25–34.
3. D. D. Streeter, Jr., H. M. Spotnitz, D. P. Patel, J. Ross, Jr., and E. H. Sonnenblick, *Fiber orientation in the canine left ventricle during diastole and systole*, Circ. Res. **24** (1969), 339-347.
4. D. D. Streeter, Jr., W. E. Powers, M. A. Ross, and F. Torrent-Guasp, *Three-dimensional fiber orientation in the mammalian left ventricular wall*, Cardiovascular System Dynamics (J. Baan, A. Noordergraaf, and J. Raines, eds.), M.I.T. Press, Cambridge, MA, 1978, pp. 73–84.
5. C. E. Thomas, *The muscular fiber architecture of the ventricles of hog and dog hearts*, Amer. J. Anatomy **101** (1957), 17–57.
6. C. S. Peskin, *Fiber-architecture of the left ventricular wall: an asymptotic analysis*, Comm. Pure Appl. Math. **42** (1989), 79–113.
7. C. S. Peskin and D. M. McQueen, *A three-dimensional computational method for blood flow in the heart.* (I) *Immersed elastic fibers in a viscous incompressible fluid*, J. Comput. Phys. **81** (1989), 372–405.
8. D. M. McQueen and C. S. Peskin, *A three-dimensional computational method for blood flow in the heart.* (II) *Contractile fibers*, J. Comput. Phys. **82** (1989), 289–297.
9. S. Greenberg, D. M. McQueen, and C. S. Peskin, *Three-dimensional fluid dynamics in a two-dimensional amount of central memory*, Wave Motion: Theory, Modeling, and Computation (Proc. Conf. in Honor of the 60th Birthday of Peter D. Lax) (A. J. Chorin, ed.), Springer-Verlag, New York, 1987, pp. 85–146.
10. C. S. Peskin and D. M. McQueen, *Modeling prosthetic heart valves for numerical analysis of blood flow in the heart*, J. Comput. Phys. **37** (1980), 113–132.
11a. C. Tu, *A study of stability in the computation of flows with moving immersed boundaries: a comparison of three methods*, thesis, New York University, 1989.
11b. C. Tu and C. S. Peskin, *Stability and instability in the computation of flows with moving immersed boundaries*, SISSC (to appear).
12. C. S. Peskin, *Flow patterns around heart valves: A digital computer method for solving the equations of motion*, thesis, Albert Einstein College of Medicine, July, 1972. (University Microfilms #72–30, 378. 211pp.)
13. ——, *Numerical analysis of blood flow in the heart*, J. Comput. Phys. **25** (1977), 220–252.
14. Leonardo da Vinci, in *Leonardo da Vinci on the human body* (C. C. O'Malley and J. B. de C. M. Saunders, eds.), Henry Schuman, New York, 1952, pp. 258–275.
15. C. S. Peskin, *The fluid dynamics of heart valves: experimental, theoretical, and computational methods*, Ann. Rev. Fluid Mech. **14** (1982), 235–259.
16. J. S. Meisner, D. M. McQueen, Y. Ishida, H. O. Vetter, U. Bortolotti, J. A. Strom, R. W. M. Frater, C. S. Peskin, and E. L. Yellin, *Effects of timing of atrial systole on LV filling and mitral valve closure: computer and dog studies*, Amer. J. Physiol. **249** (1985), H604–H619.
17. D. M. McQueen, C. S. Peskin, and E. L. Yellin, *Fluid dynamics of the mitral valve: physiological aspects of a mathematical model*, Amer. J. Physiol. **242** (1982), H1095–H1110.

18. D. M. McQueen and C. S. Peskin, *Computer-assisted design of pivoting disc prosthetic mitral valves*, J. Thorac. Cardiovasc. Surg. **86** (1983), 126–135.
19. ——, *Computer-assisted design of butterfly bileaflet valves for the mitral position*, Scand. J. Thor. Cardiovasc. Surg. **19** (1985), 139–148.
20. M. Born and J. R. Oppenheimer, Ann. D. Phys. **84** (1927), 457–484.
21. R. P. Feynman, R. B. Leighton, and M. Sands, *The Feynman lectures on physics*, Addison-Wesley, Reading, MA, 1963, pp. 40.7–40.10.
22. C. S. Peskin and T. Schlick, *Molecular dynamics by the backward-Euler method*, Comm. Pure Appl. Math. **42** (1989), 1001–1031.
23. T. Schlick and C. S. Peskin, *Can classical equations simulate quantum-mechanical behavior? A molecular dynamics investigation of a diatomic molecule with a Morse potential*, Comm. Pure Appl. Math. **42** (1989), 1141–1163.
24. C. S. Peskin, *Analysis of the backward-Euler/Langevin method for molecular dynamics*, Comm. Pure. Appl. Math. **43** (1990), 599–645.
25. R. P. Feynman, R. B. Leighton, and M. Sands, *The Feynman lectures on physics*, Addison-Wesley, Reading, MA, 1963, pp. 41.6–41.7.
26. J. A. McCammon and S. C. Harvey, *Dynamics of proteins and nucleic acids*, Cambridge Univ. Press, 1987.
27. T. Schlick, B. E. Hingerty, C. S. Peskin, M. L. Overton, and S. Broyde, *Search strategies, minimization algorithms, and molecular dynamics simulations for exploring conformational spaces of nucleic acids*, Theoretical Biochemistry and Molecular Biophysics (D. L. Beveridge and R. Lavery, eds.), Adenine Press, 1990, pp. 39–58.

COURANT INSTITUTE OF MATHEMATICAL SCIENCES, NEW YORK UNIVERSITY, 251 MERCER STREET, NEW YORK, NEW YORK 10012